

Physical nature of complex structural relaxation in polysiloxane – PMpTS: α and α' relaxations

A. Patkowski^a, J. Gapinski^a, T. Pakula^b, G. Meier^{c,*}

^a *Institute of Physics, A. Mickiewicz University, Umultowska 85, 61-614 Poznan, Poland*

^b *Max-Planck-Institute für Polymerforschung, Ackermannweg 10, 55128 Mainz, Germany*

^c *Institut für Festkörperforschung, Forschungszentrum Jülich, Postfach 1913, 52425 Jülich, Germany*

Received 23 January 2006; received in revised form 9 May 2006; accepted 10 May 2006

Available online 30 June 2006

Abstract

Structural relaxation processes in poly(methyl-*para*-tolyl-siloxane) (PMpTS) polymers of three molecular weights were studied using dynamic light scattering. Two relaxation processes: the usual α and an additional slow one α' were observed and studied as function of temperature and molecular weight. Contrary to the structural relaxation, we find that in a plot $T-T_g$ the relaxation times for the α' process for all molecular weights do not collapse to a single curve. For one of the samples the light scattering correlation functions were compared with the corresponding functions obtained by means of mechanical relaxation, dielectric spectroscopy and computer simulations. The simulations show that the bimodal distribution, i.e. the α relaxation and the slow (α') process are contained in the correlation functions of most of the probes (optical anisotropy, dipole moment, chain bond, density) in agreement with experimental observations.

© 2006 Elsevier Ltd. All rights reserved.

Keywords: Amorphous polymers; Poly(methyl-*para*-tolyl-siloxane); Computer simulation

1. Introduction

The most drastic change in the macroscopic behaviour of amorphous polymers occurs at the “glass transition”, at which the material transforms from a hard solid to a viscoelastic fluid when heated and from the fluid to the glass when cooled. The transition is related to changes in dynamics and it is well established that the segmental mobility, which allows a global flow of the system is activated at this transition. Related macroscopic effects can be detected using various experimental methods from which the mechanical, dielectric and photon correlation spectroscopies are the ones most frequently used.

Unfortunately, any interpretation of the experimental results is still purely phenomenological. It consists mainly in comparing temperature dependencies of the relaxation rates detected by various methods but to a smaller extent in a quantitative

comparison of direct interrelations between the relaxation spectra. Structural models which would allow a more precise interpretation are still missing. This makes problems in comparing the results from different experiments, which are sensitive to various microscopic effects on the segmental size scale. The most prominent and the most general is the mechanical effect, which is sensitive to segmental translations. The mechanical modulus of the purely amorphous polymers drops at the transition by three to four orders of magnitude and the related stress relaxation can be detected with a high precision. The situation is not so convenient in the case of the dielectric effects for which permanent dipole moments, which can be assigned to polymer segments, are necessary. In the case of the light scattering, depending on the experiment geometry and on the type of the optical polarisability one detects density or orientation relaxations.

Phenomenologically, the experimental data from different methods can be unified in such a way that they represent correlation functions describing relaxation of quantities characteristic for these methods. The question arises, how they can be

* Corresponding author. Tel.: +49 2461613567; fax: +49 2461612280.

E-mail address: g.meier@fz-juelich.de (G. Meier).

compared in order to give more insight in the relaxation mechanisms related to the transition. Because of lack of related theoretical descriptions, we analyse in this paper the experimental results in comparison with the computer simulation results, from which we get ideas about possible relations between various dynamic correlations detected by different methods. In polymers above the glass transition temperature T_g usually a single broad process is observed, which is attributed to the segmental motion of a polymer chain and is called the α relaxation. In the time domain it is expressed by the stretched exponential Kohlrausch–Williams–Watts (KWW) function.

In 1965 Baur and Stockmayer [1] reported unusual features of dielectric relaxation spectra of bulk poly(propyleneoxide)s, PPO. They found a small secondary loss peak at the long time shoulder of the α process, the position of which was strongly dependent on the molecular weight of the polymer. Processes of this kind will be called α' relaxation in this paper. Depending on the measured quantity and the structure of the polymer chain, several physical processes could be attributed to the α' relaxation. In the case of PPO [1], application of the Rouse–Bueche–Zimm theory [2–4] allowed to attribute that additional process to the chain normal modes. In the discussion Baur and Stockmayer stressed the fact that the structure of poly(propyleneoxide) (presence of the methyl side group) causes the monomer dipole moment to deviate slightly from the direction perpendicular to the chain contour, which produces a small dipole moment component parallel to it. Summation over all monomers gives a resultant dipole moment of that component proportional to the end-to-end distance vector of the polymer. For such long-range conformational relaxation the Rouse–Bueche–Zimm theory was found to be most adequate. Since in such conditions practically only the second normal mode is visible in dielectric relaxation, Baur and Stockmayer analysed the two extremes: (i) for undiluted polymers, after assuming “free-draining” conditions, they arrived at Bueche’s and Rouse’s formula [2,3] for the characteristic time of the second normal mode τ_2 :

$$\tau_2 = \frac{3M\eta}{\pi^2\rho RT} \quad (1)$$

where M is the molecular weight of the polymer, ρ its density, η is the viscosity, and RT has its usual meaning and (ii) for diluted polymers (“non-draining” limit) one should rather use Zimm’s result [4]. The formula predicts the M -dependence of τ_2 as $\tau_2 \propto M^2$, since $M \propto \eta$ in the Rouse regime for $M < M_c$, the critical molecular weight. The experimental results fit well within the region defined by the Rouse and Zimm predictions. They used polymers of molecular weights of 1025–5000 g/mol, the ratio of relaxation times of the α' to the α mode amounted to approximately 100–2000 (increasing with the molecular weight).

In 1976 Yano et al. [5] reported new dielectric data on PPO in bulk and solutions in methylcyclohexane. The dielectric relaxation (DR) measurements were performed in a very broad range of frequencies ($\log f_{\max}$ (Hz) = –3 to 9.5) and were

combined with Brillouin scattering. The authors focused on the primary (segmental) relaxation process and investigated its behaviour at different concentrations for two molecular weights ($M_w = 2025$ and 4000 g/mol). From the data and discussion presented in the paper it is hard to tell, if the dielectric loss spectra consisted of two peaks.

The theory of the influence of internal polymer modes on the correlation function of scattered light is still not complete. Pecora [6] gave an analytical solution for the case of large ($qR_g > 1$) non-interacting coils but only for the case of polarised scattering. The general conclusion is that the complete correlation function is a sum of terms containing subsequent normal mode characteristic times, starting from the “0” mode, that is rotation of the whole coil. The amplitudes of all terms are q -dependent: the first one decreases, while all the others increase with increasing q values. What is worth mentioning, for $qR_g < 1$ the contribution of all the internal terms is practically negligible.

The depolarised scattering for the Rouse–Zimm dynamical model of flexible polymer chains is a much more challenging problem. It was calculated by Ono and Okano for the special case of $q = 0$ [7]. As a result they obtained a spectrum of Lorentzians, each with a relaxation time characteristic for one of the Rouse–Zimm modes. However, the contribution of each mode to the spectrum was equal.

To our knowledge there is no other theory concerning the depolarised dynamic light scattering spectrum of polymer chain internal modes.

In 1976 Jones and Wang [8] presented data on depolarised Rayleigh scattering from bulk and diluted poly(propylene glycol), PPG. Only a single relaxation process (well fitted to a Lorentzian function) was found in the experimental temperature range. Its characteristic time was strongly concentration dependent and molecular weight independent, as was previously found for the segmental motion. In 1981 Wang et al. [9] performed dynamic light scattering studies on bulk and diluted PPG. A single stretched exponential (KWW) function fitted well the measured correlation functions and the conclusion was that Rouse–Zimm modes observed by Baur and Stockmayer [1] were not active in light scattering. Johari in 1986 [10] reports DR studies on a PPO sample of $M_w = 4000$ g/mol. He was able to follow two relaxation processes above T_g . The faster process visible above T_g was attributed to segmental motion of the backbone (α relaxation), whereas the slower one to the normal mode relaxation (α' process), although no attempts were made to compare the relaxation times with theoretical models.

Two papers by Adachi and Kotaka [11,12] describe dielectric relaxation of *cis*-poly(isoprene), PI of different molecular weights $M_w = 1000$ to 128,000 g/mol. They found both α and α' relaxations, α being almost molecular weight independent and α' being strongly molecular weight dependent.

In 1989 Boese et al. [13] reported simultaneous DR and photon correlation spectroscopy (PCS) measurements on narrowly distributed bulk poly(methylphenylsiloxane), PMPS of $M_w = 28,500$ g/mol. Apart from the main conclusion of the paper that correlation times of the α process obtained with

both methods are the same, another important feature of the system was found. The authors report that the PCS correlation functions contain an additional mode, slower than the segmental one and of comparable or larger width. The correlation times of this process obtained from the polarised (VV) and depolarised (VH) correlation functions were approximately equal. The separation in time (judged from the plots) between the two processes was of the order of 2.5–3 decades. The DR spectra for the same sample contained only one loss peak without any indication of the presence of the slower one. The slow process in the correlation functions obtained from the light scattering experiments was attributed to the normal mode as in the case of previously cited reports on PPO and PI, although here, for the first time to our knowledge, it had been probed by a light scattering technique. The absence of the α' relaxation in DR spectra was explained by the symmetry of the Si–O bond, which caused that there was no dipole component parallel to the chain contour. This was a severe condition for activating normal modes in DR experiments in the case of PPO and PI. This is probably the reason why we were not able to find any DS data on α' process in poly(siloxane)s in literature.

In 1994 and 1995 there appeared two papers by Kanaya et al. [14,15] devoted to the problem of clusters in glass-forming polymers. The light scattering measurements (static and dynamic) were performed on a poly(methyl-*para*-tolyl-siloxane) (PMpTS) sample of $M_w = 15,000$ g/mol. As in the previous case, apart from the dominant segmental relaxation, another, slower and broader process was found both in the polarised and depolarised PCS spectra. Since it was not the main problem under study, the physical origin of this slow relaxation was not discussed, and only its similarity to the one in the work of Boese et al. [13] was mentioned. From the numerical analysis (double KWW fit, see below) of the experimental data, Kanaya et al. [14,15] gave estimated values of the relaxation times and KWW β -parameters of the slow mode.

Since it has not been clarified, what was the origin of the slow process in both poly(siloxane) samples, we decided to perform a PCS study on PMpTS samples of different molecular weights combined with dielectric and mechanical relaxation measurements. Computer simulations of different processes in polymer chains, recently successfully applied by Pakula et al. [16–18] to complex polymer systems, were also used to help interpret the experimental data.

2. Materials

Dynamic light scattering experiments were performed on two poly(methyl-*para*-tolyl-siloxane) (PMpTS) samples of molecular weights $M_w = 4500$ and $42,000$ g/mol, respectively. Polydispersity indices (M_w/M_n) measured by means of gel permeation chromatography (GPC) amounted to 1.16 and 1.11, respectively. Glass transition temperatures T_g determined by differential scanning calorimetry (DSC) measurements at the cooling rate of 10 K/min were -26 and -17 °C, respectively. For data interpretation we used also previously obtained results on the $M_w = 15,000$ g/mol sample, the preparation

and characteristics of which have been described in detail before [14].

All three samples were synthesized in the same laboratory (MPI-Polymerforschung, Mainz, chemical lab) using the same technique of anionic polymerisation. After synthesis, the light scattering samples of molecular weights of 4500 and 42,000 g/mol were prepared by extensive drying of solutions in *n*-hexane in the presence of molecular sieves, then filtering the concentrated PMpTS solution through a 0.22 μ m Millipore filter directly into dust-free cylindrical Pyrex glass cells of 10 mm inner diameter and finally keeping under vacuum at the temperature of 100 °C for several days until all the solvent was evaporated.

3. Methods

3.1. Dynamic light scattering – photon correlation spectroscopy

The dynamic light scattering (photon correlation spectroscopy) measurements were performed in the depolarised – VH geometry, i.e. the incident beam was polarised vertically and only the horizontal (depolarised) component of the scattered light was measured. A krypton-ion laser (Spectra Physics) was the light source in the case of the 15,000 g/mol sample, and a diode pumped Nd-YAG laser (ADLAS) in the case of the two other samples. In all cases the autocorrelation function $G^{(2)}(t)$ of scattered light intensity $I(t)$ was measured with the ALV-5000 digital correlator (ALV, Langen, Germany). This intensity, $I(t)$, autocorrelation function $G^{(2)}(t) = \langle I(t)I(0) \rangle$ is related to the field, $E(t)$, autocorrelation function $g^{(1)}(t) = \langle E(t)E^*(0) \rangle$ via the Siegert relation for the homodyne case [19],

$$G^{(2)}(t) = \langle I \rangle^2 (1 + f |g^{(1)}(t)|^2) \quad (2)$$

where $\langle I \rangle$ is the mean intensity and f is an experimental factor. Data were analysed using a double KWW function as a model for $g^{(1)}(t)$

$$g^{(1)}(t) = A_z \exp \left[- \left(\frac{t}{\tau_z} \right)^{\beta_z} \right] + A_{z'} \exp \left[- \left(\frac{t}{\tau_{z'}} \right)^{\beta_{z'}} \right] \quad (3)$$

A typical fit of the experimental correlation function using Eq. (3) is shown in Fig. 1.

3.2. Mechanical relaxation

Dynamic mechanical measurements have been performed by means of the Rheometrics RMS 800 mechanical spectrometer. Shear deformation has been applied under condition of controlled deformation amplitude, always remaining in the range of the linear viscoelastic response of the samples studied. Frequency dependencies of the storage (G') and loss (G'') shear modulus have been measured at various temperatures. Geometry of parallel plates has been used with plate diameters of 6 mm and the gap between plates (sample

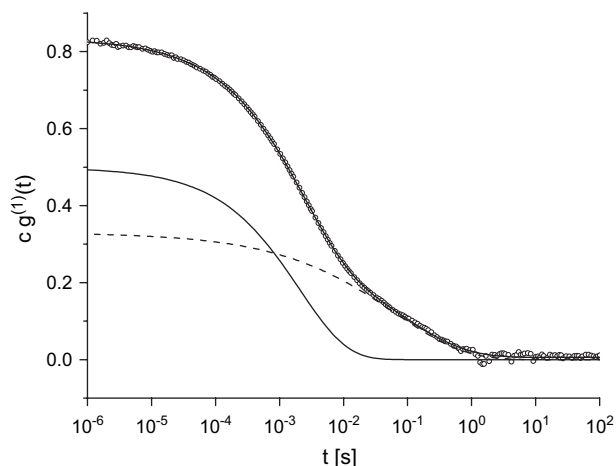


Fig. 1. Decomposition of the correlation function into two KWW components. The solid line corresponds to the α relaxation and the dashed line to the α' relaxation. The function was measured for the PMpTS sample of $M_w = 4500$ g/mol at $T = -12^\circ\text{C}$.

thickness) was about 1 mm. Experiments have been performed under dry nitrogen atmosphere.

3.3. Dielectric relaxation

The frequency and temperature dependent dielectric measurements were performed using the experimental set-up of Novo-Control. The system was equipped with an alpha high resolution dielectric analyser, the impedance analyser HP 4191A and temperature controller Quatro version 4.0. The complex dielectric modulus, $M^*(\omega) = M'(\omega) - iM''(\omega)$, has been determined in the frequency range from 10^{-2} to 10^7 Hz (Fig. 2a).

Flat parallel plate capacitor (diameter 10 mm, thickness 0.07 mm) has been used. The value of AC voltage applied to the capacitor was equal to 1 V. Temperature was controlled using a nitrogen-gas cryostat and the temperature stability of the sample was better than 0.1 K.

3.4. Computer simulations – the simulation method

Some important properties of polymers like viscosity of melts or global transport properties are uniquely determined by the topology of macromolecules, which can be represented by very simple models. There are, however, other properties, which require a consideration of polymer structures in more detail but still not with the precision considered in the molecular dynamics. The important parameters, which determine many intermediate scale properties, are the space filling requirements and internal mobilities of macromolecular elements (monomers). The latter are mainly determined by the chemical constitution and by the connectivity between atoms given by the skeleton of covalent bonds.

In this paper an attempt is made to consider these details of chemical constitution of molecules in the Monte Carlo simulation. The Cooperative Motion Algorithm (CMA) [16] is applied to simulate lattice polymers, in which the most important

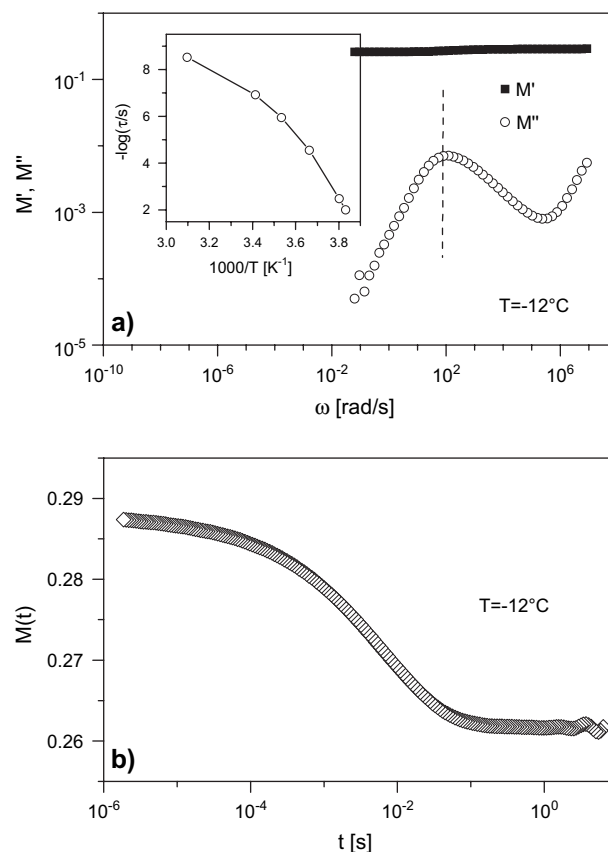


Fig. 2. (a) Frequency dependencies of the real (M') and imaginary (M'') components of the complex dielectric modulus in the frequency range of the segmental relaxation. The vertical dashed line marks the frequency taken for determination of the relaxation time of the dielectric α process. The inset shows the temperature dependencies of the segmental relaxation times. (b) Relaxation dielectric modulus determined by transformation of the dynamic dielectric spectrum presented in (a).

features of the chemical structure are taken into account, i.e. the specific skeleton of covalent bonds connecting all atoms into a monomer and finally into a polymer under condition of excluded volume. The molecules are represented by a number of beads (representing atoms) connected by non-breakable bonds in a way corresponding to the skeleton of covalent bonds joining atoms in a selected type of real molecules. Such molecular structures are organized on a lattice to a dense system under the excluded volume condition.

Macromolecules consist usually of thousands of atoms at specific positions within a complex bond skeleton characteristic for each type of the molecule. It is interesting to notice that for most of macromolecules atomic sizes and bond lengths remain within a relatively narrow range. This should allow a simplified representation of macromolecular structures, in which sizes and lengths of bonds between atoms are not distinguishable. With this approximation macromolecules can be represented on lattices as systems of beads connected by non-breakable bonds with beads considered as atoms and bonds forming structures corresponding topologically to bond skeletons of real molecules. Fig. 3 illustrates such a representation of the polymer considered in this paper.

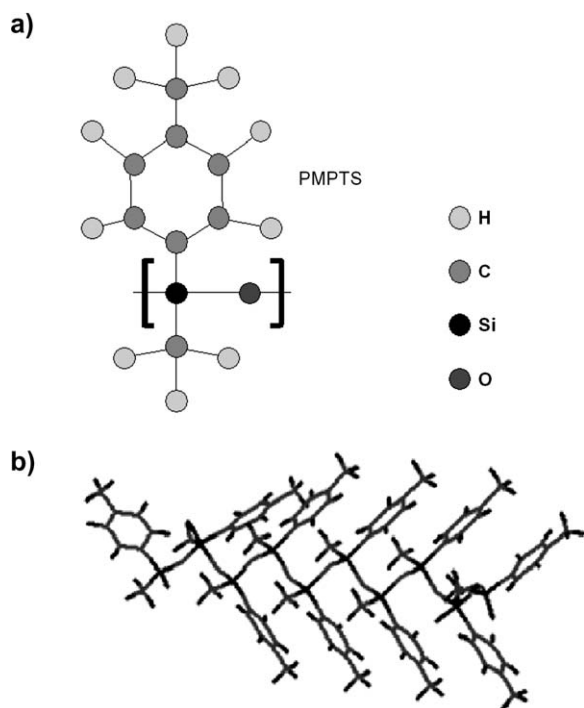


Fig. 3. Monomer (a) and polymer fragment (b) of the PMpTS, as considered in the simulation. The macromolecules are arranged on the fcc lattice with atoms at the lattice sites and the bonds along the lines connecting them. The atoms are not distinguishable in the simulation. Nearly all lattice sites are occupied by the atoms in order to represent a dense system.

Macromolecules can be quite flexible in solutions or in melts rearranging all the time in space preserving, however, the connectivity between atoms given by the bond skeleton. In order to provide lattice molecules with sufficient flexibility, we apply concepts of atomic rearrangements used previously in simulations of dense polymer systems on lattices [20,21].

In this method, sequential attempts of rearrangements of atomic groups are considered. A single attempt consists of several steps including a random choice of an atom, a random choice of the direction of its attempted displacement and a test of constraints given by bonds with neighbours and by the excluded volume condition. Examples of moves resulting from successful attempts of this kind are illustrated in other publications [20,21]. The resulting rearrangements can involve displacements of one or more atoms. They change conformation of the molecule but preserve their identity given by the specific architecture of the bond skeleton and positions of atoms within the skeleton. A large variety of rearrangements are possible and it is not possible to specify all of them.

Simulations of the macromolecular structures, shown in Fig. 3, are performed for three-dimensional systems on the fcc lattice. The lattice in all considered cases is used only as a coordination skeleton of the space. It helps to identify neighbours. Distances between lattice sites do not influence the rules of rearrangements in the a-thermal cases, as considered here. Motion of simulated molecules allows to generate a large number of states, which can be averaged to get representative information about the structure of the molecule in equilibrium.

Monitoring the structural changes and displacements of the model and its elements in time it is possible to get information about the dynamics.

Because of the complex monomer structure various processes can contribute to chain relaxation on the local scale. On the other hand, various measures of the local dynamics are possible depending on the method the dynamics is detected. As a quantitative measure of a local motion usually the autocorrelation function of a vector or tensor quantity, related to a structural element, embedded in the chain is used. Various experimental methods detect various correlations depending on the kind of a probe characteristic for a given method. Two types of the orientation correlation functions are usually considered

$$\rho^1(t) = \langle m(0) \cdot m(t) \rangle \quad (4a)$$

$$\rho^2(t) = (3\langle (m(0) \cdot m(t))^2 \rangle - 1)/2 \quad (4b)$$

where m is the vector under consideration at time 0 and t and the angular brackets denote the ensemble averages over conformational states belonging to the motional sequence within the investigated time interval.

The local dynamic properties of the model polymers considered in this paper are characterized by the following quantities:

- (1) The first order autocorrelation function of a skeletal bond

$$\rho_b^1(t) = \langle b_i(t) b_i(0) \rangle \quad (5a)$$

and corresponding second order correlation function $\rho_b^2(t)$

$$\rho_b^2(t) = \{3\langle (b_i(0) \cdot b_i(t))^2 \rangle - 1\}/2 \quad (5b)$$

where b_i are unit vectors representing the bond orientation.

- (2) The autocorrelation function characterizing reorientation of the phenyl rings

$$\rho_{Ph}^1(t) = \langle P(t) P(0) \rangle \quad (6a)$$

and corresponding $\rho_{Ph}^2(t)$

$$\rho_{Ph}^2(t) = \{3\langle [P(0) \cdot P(t)]^2 \rangle - 1\}/2 \quad (6b)$$

with the vectors $P(0)$ and $P(t)$ normal to the ring at time $t = 0$ and t , respectively.

- (3) The segmental position autocorrelation function characterizing the local translation mobility of systems

$$\rho_c(t) = \langle c_i(0) c_i(t) \rangle \quad (7)$$

where $c_i = 1$ for a bead belonging to a given monomer, if its position at time t overlaps with the position occupied by the monomer at $t = 0$ and $c_i = 0$, when a bead is displaced from such position.

- (4) The correlation function describing dipole orientation relaxation

$$\rho_{\text{dip}}(t) = \langle \mu_i(0) \mu_j(t) \rangle \quad (8)$$

where μ_i are vectors along the bisectors of the Si–O–Si angles in the backbone and thus contain components parallel and perpendicular to the main chain bonds.

4. Results

4.1. PCS

PCS measurements were performed in the VH configuration in order to avoid the effects of stray light or strong scattering from clusters that sometimes might appear in the samples [14]. It has been proven experimentally that the relaxation times obtained from VV and VH correlation functions are almost the same. The temperature range was adjusted for each sample in such a way that the relaxation times fit into the correlator window, i.e. from about 2 to 25 °C above T_g . The mean KWW times were calculated according to the formula

$$\langle \tau_{\text{KWW}} \rangle = \frac{\tau_{\text{KWW}}}{\beta_{\text{KWW}}} \Gamma(\beta_{\text{KWW}}^{-1}) \quad (9)$$

where $\Gamma(x)$ is the gamma function and τ_{KWW} and β_{KWW} for each process were obtained from fitting Eq. (3) to the experimental data.

Results showing the temperature dependence of $\langle \tau_{\alpha} \rangle$ and $\langle \tau_{\alpha'} \rangle$ for all three PMpTS samples are presented in Fig. 4. In order to account for the T_g differences, we plot the same data as a function of $T - T_g$ (Fig. 5) assuming the same viscosity at the same distance from T_g for all samples measured. It is clearly seen that the curves corresponding to the faster (α) process overlap quite well and those representing the slower one (α') are still well separated in time. The distance between the α relaxation master curve and the slower process is an increasing function of the polymer molecular weight. The ratio of

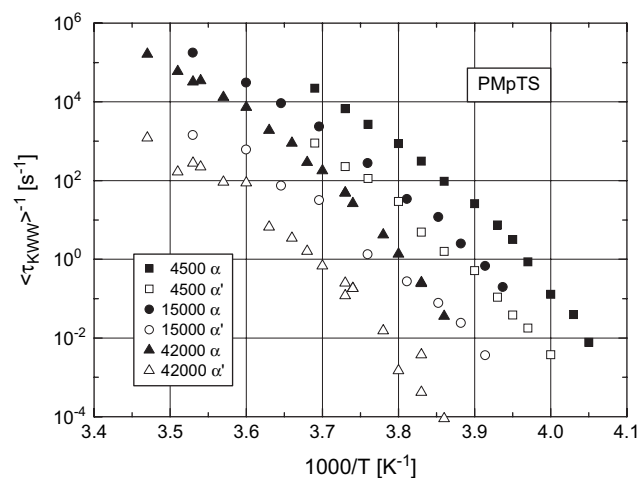


Fig. 4. Temperature dependence of both relaxation processes (α and α') in all three PMpTS samples of indicated molecular weights.

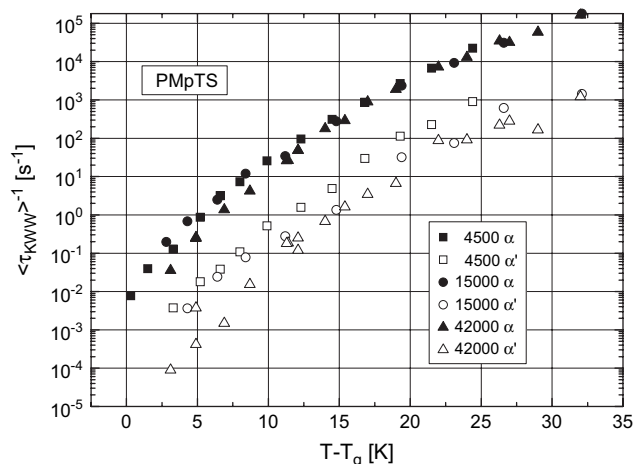


Fig. 5. The same data as in Fig. 4, but corrected for T_g .

α' relaxation times of the 42,000 and 4500 molecular weight samples at the same $T - T_g$ values is of the order of 10. We think that an important feature of the poly(siloxane)s is a quite narrow distribution of relaxation times corresponding to the α relaxation, which makes the separation of the α and α' processes possible.

In Fig. 6 the temperature dependence of the KWW β -parameter for all three samples is shown. Note that the values of the β -parameter corresponding to the α relaxation amount to 0.6–0.7 and apparently increase with increasing molecular weight, as well as with increasing temperature. The values of the β -parameter corresponding to the α' relaxation seem to be temperature independent and tend to decrease with increasing polymer molecular weight. The lack of noise in the $\beta_{\alpha'}$ data in Fig. 6 is caused by the fitting procedure. Since in double KWW fits there are six independent parameters for a zero baseline, the fitting procedure included preliminary calculations for all temperature points with all parameters free and then the mean value of $\beta_{\alpha'}$ was used in final fits as a fixed parameter. Such a procedure brings more confidence to the values of other fit parameters, e.g. the times and amplitudes

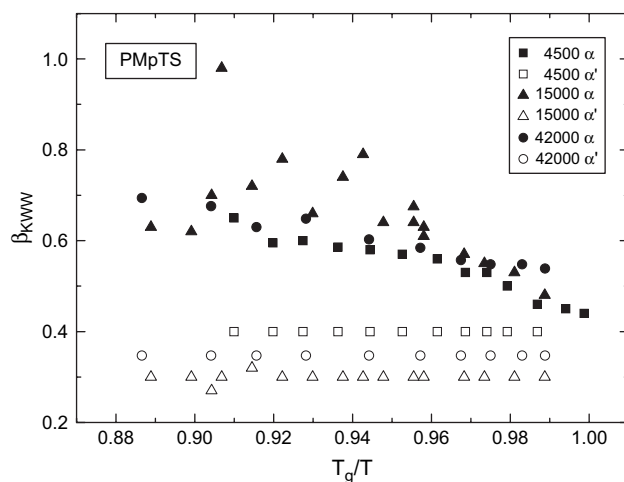


Fig. 6. Temperature dependence of the KWW β -parameters of the α and α' processes for all three PMpTS samples.

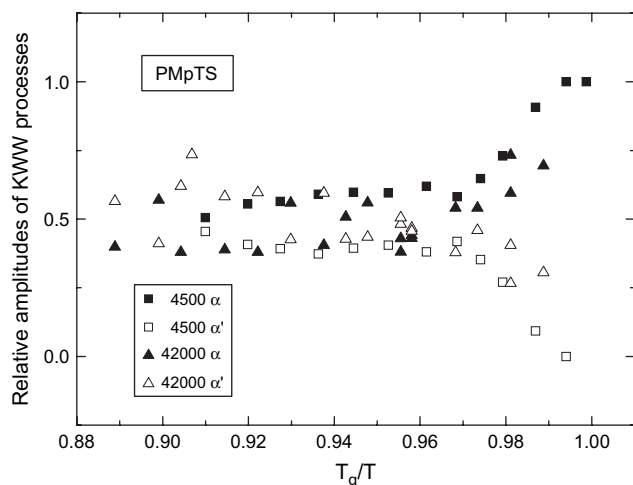


Fig. 7. Temperature dependence of the relative amplitudes of the α and α' KWW components for two PMpTS samples of indicated molecular weights.

of the two components. The temperature dependence of the relative amplitudes (normalized so that $A_\alpha + A_{\alpha'} = 1$) for the samples of $M_w = 4500$ and $42,000$ g/mol is presented in Fig. 7.

4.2. Mechanical relaxation

The frequency dependencies of G' and G'' , measured within the frequency range of 0.1 – 100 rad/s at various temperatures, have been used to construct master curves representing the broad range frequency dependencies of these quantities. Only shifts along the frequency scale have been performed. An example of such master curve is presented in Fig. 8a. This procedure provided a temperature dependence of shift factors ($\log a_T$ versus T). The master curves of G' and G'' allow to distinguish two relaxation processes. The relaxation time in the glassy range at high frequencies at the reference temperature has been determined as $\tau(T_{\text{ref}}) = 1/\omega_c$, where ω_c is the frequency at which the G' and G'' curves cross each other. Analogously, the relaxation time of the slow process attributed to the polymer chain relaxation (τ_c) has been determined from the cross point of the characteristic frequency dependencies of $G' \sim \omega^2$ and $G'' \sim \omega$ (dashed lines in Fig. 8a) extrapolated from the low frequency Newtonian flow range to higher frequencies (see the vertical arrows). Relaxation times at other temperatures are given by $\log \tau(T) = \log \tau(T_{\text{ref}}) + \log a_T$. The temperature dependencies of the segmental (τ_s) and chain (τ_c) relaxation times are shown in the inset of Fig. 8a. The temperature dependence of the segmental relaxation time is fitted by the Williams–Landel–Ferry (WLF) relation $\log a_T = C_1(T - T_g)/(C_2 + T - T_g)$, where C_1 and C_2 are constants (dashed line), which meet the T_g value (determined by DSC) at the time of 100 s as often observed for amorphous polymers.

In order to have a possibility to compare the results of these measurements with time dependent correlations, determined in other experiments, the frequency spectra of the mechanical behaviour have been transformed to the time domain yielding the relaxation modulus $G(t)$ shown in Fig. 8b. Fitting the

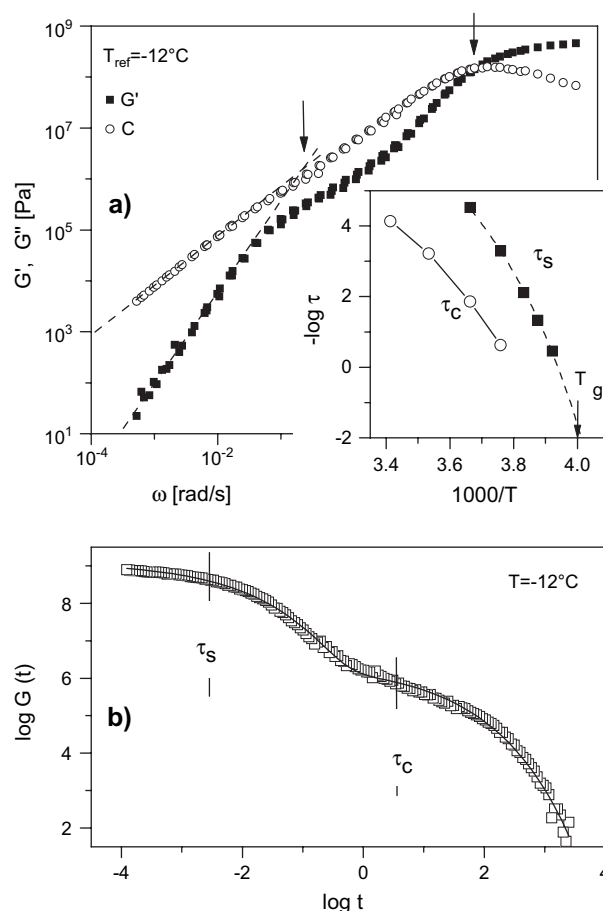


Fig. 8. (a) Frequency dependencies of the real (G') and imaginary (G'') components of the complex shear modulus (master curves). The vertical arrows mark frequencies taken for determination of the relaxation times of the segmental and chain motions. The dashed lines with slopes 1 and 2 correspond to the characteristic frequency dependence for the Newtonian flow range behaviour of the G'' and G' , respectively. The inset shows the temperature dependencies of the segmental and chain relaxation times. (b) Relaxation shear modulus by transformation of the dynamic mechanical results presented in (a). The solid line shows the fit of the sum of two stretched exponential functions.

relaxation modulus function with the sum of two stretched exponential processes, resulted in comparable values of the average relaxation times as these were determined from the frequency dependencies of G' and G'' .

4.3. Dielectric relaxation

Relaxation times have been determined from maximum positions in M'' ($\tau = 1/\omega_{\text{max}}$). Because of the broad frequency range accessible for this method, the relaxation times were determined directly from measurements at various temperatures. An example of the temperature dependence of the relaxation times is presented in the inset of Fig. 2a. In analogy to the processing of the mechanical data, the complex dielectric modulus has been transformed to the dielectric relaxation modulus as shown in Fig. 2b. In a recent paper by Mpoukoulas and Floudas [22] DR spectra of PMpTS as a function of pressure and temperature have been reported. These authors

analyse their data by Havriliak–Negami functions, yielding a similar Arrhenius plot as in our case.

4.4. Computer simulation results

Using the MC computer simulation method the following correlation functions were calculated: (i) the first order bond orientation correlation function $\rho_b^1(t)$, Eq. (5a); (ii) the second order bond orientation correlation function $\rho_b^2(t)$, Eq. (5b); (iii) the first order dipole orientation correlation function $\rho_\mu^1(t)$, Eq. (8); (iv) the second order orientation correlation function of the phenyl rings $\rho_{Ph}^2(t)$, Eq. (6b); (v) the first order orientation correlation function of the phenyl rings $\rho_{Ph}^1(t)$, Eq. (6a); and (vi) the position correlation function characterizing the translation mobility of the system the second order orientation correlation function of the phenyl rings $\rho_c^1(t)$, Eq. (7). All these correlation functions are shown in Fig. 9 for comparison. As it is evident from Fig. 9, additional slow relaxations are clearly visible in the orientation correlation functions of the bond vector ((i) and (ii)) and in the position correlation function (vi). All these correlation functions were calculated without taking into account any interactions (except connectivity of the polymer chain), which could lead to the cooperative dynamics of the neighbouring monomers and to cooperative dynamics.

5. Discussion

Although many aspects apparently support the assignment of the slower (α') mode to the superposition of the polymer chain normal modes, it is not quite clear, if the normal modes can be visible in light scattering for such small polymers. Both available theories (for polarised and depolarised correlation functions) deal only with the case, where qR_g is greater than one. Certainly this is not the case both for our PMpTS and Boese's PMPS sample. For smaller q 's no other mode, except overall diffusion is predicted.

Comparison of the first order correlation functions obtained by means of dynamic light scattering, dielectric and mechanical relaxation is presented in Fig. 10.

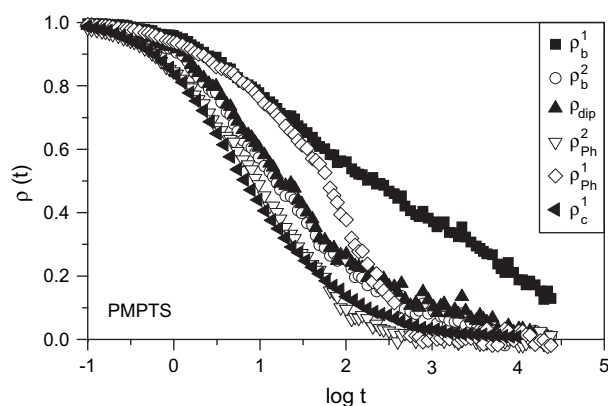


Fig. 9. Simulated correlation functions: \blacksquare – $\rho_b^1(t)$, Eq. (5a); \circ – $\rho_b^2(t)$, Eq. (5b); \blacktriangle – $\rho_{dip}(t)$, Eq. (8); ∇ – $\rho_{Ph}^2(t)$, Eq. (6b); \diamond – $\rho_{Ph}^1(t)$, Eq. (6a); and \blacktriangleleft – $\rho_c^1(t)$, Eq. (7).

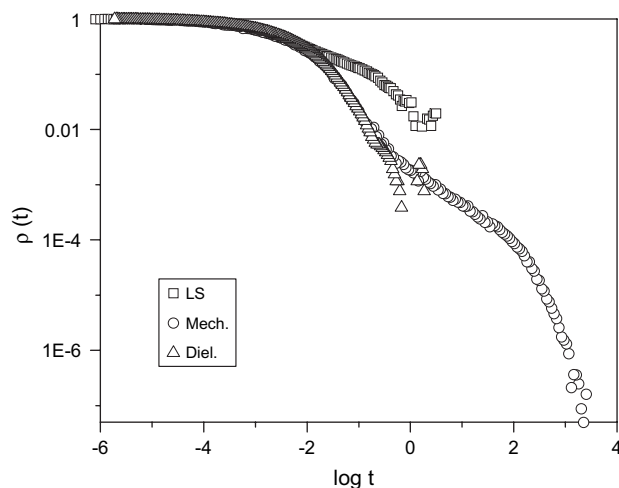


Fig. 10. First order correlation functions obtained from DLS, MR and DS experiments.

The α relaxation (initial decay of the correlation functions) measured by all three experimental techniques is almost identical, indicating that in all cases the same local segmental relaxation is probed. It is clearly seen that the chain dynamics probed by mechanical relaxation (second part of the decay of the correlation function) is about two decades slower than the α' process probed by PCS. The dielectric spectra, as in the case of PMPS, showed only one relaxation process, attributed to segmental motion of the polymer chain.

The comparison of the experimental and simulated correlation functions may help to identify the physical nature of the α' process. The DLS correlation function decays initially due to the α process in a similar way, as the other two correlation functions. At longer times a much slower α' process can be seen. The main contribution to this correlation function of the depolarised component of scattered light comes from the phenyl rings which have high optical anisotropy. Another weaker contribution (lower optical anisotropy) is due to the polymer chain backbone. It has been shown [23] that the effective optical anisotropy per monomer in PMPS, a chemically similar polymer, is higher than that of isolated monomer, indicating the presence of static orientation correlations of the phenyl rings in this polymer. These orientation correlations contribute also to the DLS correlation functions which, in this case, measure more cooperative dynamics of the PMpTS and PMPS chains, which might be assigned to the α' process.

The simulated first order correlation function of the phenyl rings, $\rho_{Ph}^1(t)$, in Fig. 9 exhibits clearly two processes: the α relaxation and additionally a slower process which can be related to the α' relaxation. The additional weak contribution to the DLS correlation function due to the relaxation of the optically anisotropic backbone will resemble the orientation correlation function of the backbone bonds $\rho_b^1(t)$ in Fig. 8.

The DLS correlation function resembles the one obtained by mechanical relaxation (MR) in terms of time distribution of the relaxation processes observed in the time range, where both correlation functions were measured. The difference in the entire shape of these two correlation functions, i.e. the

fact that it is not possible to superimpose them, may be due to different amplitudes of different contributions in the DLS and MR experiments.

The MR correlation function contains information on all dynamic processes leading to the motion of the chain and can be compared with the simulated bond orientation correlation function $\rho_b^1(t)$ in Fig. 9. The correlation function contains contributions due to the α relaxation and slower processes. Since the amplitude of the combined correlation function obtained from MR spans about seven orders of magnitude (i.e. much more than the correlation functions obtained from the other two methods), it contains information on even slower processes than those seen in DLS experiment.

The experimental correlation function obtained by means of dielectric spectroscopy (DS) contains information only on the α relaxation and the α' relaxation cannot be seen. This may be due to the fact that the component of the dipole moment of the elementary relaxing unit parallel to the chain backbone is almost zero.

The temperature dependence of the relaxation times of the α and α' relaxations obtained from DLS, MS and DS experiment is shown in Fig. 11. As one can see, the relaxation times of the α processes obtained from all three methods are very similar in the entire temperature range studied. The small differences between them might be due to the different correlation functions measured (different probes) and due to difficulties in the decomposition of the experimental functions into two overlapping KWW contributions.

The relaxation times of the α' relaxations obtained from DLS are always about two orders of magnitude shorter than those obtained from MR. This might be due to the cut-off of the DLS correlation functions at long times resulting from a much smaller amplitude range covered. Simply speaking, the very slow processes of a very low relative amplitude lower than 0.01 disappear in the background noise of the correlation function.

Another important information that can lead to a better understanding of the physical nature of the α' relaxation in

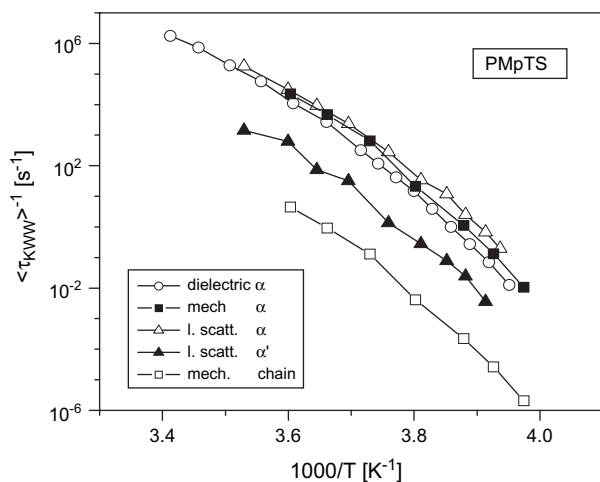


Fig. 11. Comparison of PCS, dielectric, and mechanical results for the PMpTS sample of $M_w = 15,000$ g/mol.

poly(siloxane)s is the molecular weight dependence of the relaxation times of the α and α' relaxations. In Fig. 5 the values of the α' relaxation times for the sample of $M = 15,000$ g/mol are more or less similar to that of the $M = 42,000$ g/mol sample. This may be due to the fact that the so-called critical molecular weight is between these two molecular weights and probably close to the one of PMPS being about 37,000 g/mol, as was outlined by Momper [24] in analogy to the PS, *p*-tolylPS system. Accordingly then, we have to compare α' relaxation times for samples of molecular weights of $M = 4500$ with $M = 15,000$ g/mol (below M_c), which are different approximately by a factor of 3. These measured correlation times of the α' processes fulfil the prediction of the Rouse model (cf. Eq. (1)). For relaxation time values close to T_g those relationships are not that clearly seen, because the experimental error is much larger due to the fact that the α' process is at the long time end of the correlation function and there partially outside the experimental time window.

6. Conclusions

The dynamics of PMpTS of three different molecular weights was studied by means of dynamic light scattering – photon correlation spectroscopy and compared, for one molecular weight, with results obtained from mechanical relaxation, computer simulations and dielectric relaxation.

The correlation function measured by means of DLS exhibits two relaxation processes: the usual segmental mode (α relaxation) and an additional slow process due to more cooperative chain modes (α' relaxation). The slow process was also seen in mechanical relaxation data. It is not present in dielectric spectroscopy data, probably due to the fact that the dipole moment of the relaxing subunit has no component parallel to the chain backbone. Both α and α' processes obtained from DLS exhibit a VFT temperature dependence. When plotted versus $T - T_g$, the relaxation times of the α process collapse on a master curve, while the separation between the α and α' relaxation times increases with increasing molecular weight. The molecular weight dependence of the α' relaxation times for samples below the entanglement molecular weight is given within the experimental uncertainty by the Rouse–Bueche prediction.

The reason that an additional slow α' process is seen in the DLS correlation functions of PMpTS and PMPS might be that there exist substantial orientation correlations between the phenyl rings in these polymers and that these correlations contribute to the effective optical anisotropy. These fluctuations are measured in the DLS experiment and thus allow to monitor a more cooperative dynamics of the polymer chain. Additionally, the β_{KWW} stretching parameter of the α relaxation is in this case relatively high (about 0.6), making possible the separation of the α and α' processes.

The experimental first order correlation functions obtained from DLS, MR and DS were compared for a single molecular weight sample at one temperature. They overlap in the α relaxation time range. The slow process in the DLS correlation function is about two orders of magnitude faster than that in

the MR correlation function. However, it is not excluded that the correlation functions obtained from DLS and MR, in the time range where both are defined, contain similar contributions but with different amplitudes, what results in the different shape. An additional reason for this difference might be that the MR correlation function amplitude covers about seven orders of magnitude while that of DLS covers only two to three orders of magnitude. Thus, it is possible that in the DLS data, the slowest process of the lowest amplitude disappears in the baseline noise. A similar argument might hold also for the DS correlation function.

The broad bimodal distribution of the relaxation times can be seen also in the following correlation functions obtained from computer simulations: (i) first order orientation correlation function of the backbone bonds $\rho_b^1(t)$ which can be probed in the MR experiment; (ii) second order bond orientation correlation function $\rho_b^2(t)$; (iii) first order orientation correlation function of the phenyl rings $\rho_{ph}^1(t)$ probed by depolarised light scattering; (iv) orientation correlation function of the dipole moment having a component parallel to the chain, which is measured in a DR experiment; and (v) the density correlation function. Obviously, the slow process is better visible in the first order correlation functions. Thus, the simulations show that the bimodal distribution, i.e. the α relaxation and the slow (α') process are contained in the correlation functions of most of the probes (optical anisotropy, dipole moment, chain bond, density) in agreement with experimental observations. Consequently, the slower α' process seems to be a general feature of PMpTS and PMPS dynamics and shows up in the correlation functions of the backbone bonds and phenyl ring orientations or density fluctuations obtained from computer simulations at times longer than the α process. The observability and separation of these two processes depend on the probe and experimental method used. Thus, we can obtain this slow process in the computer simulations without additionally introducing new processes like the relaxation of the end-to-end vector of the polymer chain.

In our previous work [25] we studied the combined effects of temperature and pressure on the α and α' relaxations in poly(methylphenylsiloxane) (PMPS). We found that the pressure dependence of the characteristic temperatures, dT_g/dP and dT_α/dP , and the values of the activation volume ΔV^\ddagger were very similar for both processes. Also the scaling of the combined temperature and pressure dependence of the relaxation times of both processes can be done using the parameter $\Gamma = \rho^n/T$ with the same value of the exponent n . These features

also indicate that both α and α' processes are due to the relaxation of a similar molecular subunit but with a different cooperativity.

Acknowledgements

Partial financial support from the Polish Ministry of Scientific Research and Information Technology (grant No. 1 PO3B 083 26) and “SoftComp” Network of Excellence (No. S080118) is gratefully acknowledged. Special thanks are due to Dr. Stefan Kahle, a co-worker of the late Prof. Pakula, who provided us with important information about Fig. 9.

References

- [1] Baur ME, Stockmayer WH. *J Chem Phys* 1965;43:4319–25.
- [2] Rouse PE. *J Chem Phys* 1953;21:1272–80.
- [3] Bueche F. *J Chem Phys* 1952;20:1959–64.
- [4] Zimm BH. *J Chem Phys* 1956;24:269–78.
- [5] Yano S, Rahalkar RR, Hunter SP, Wang CH, Boyd RH. *J Polym Sci, Polym Phys Ed* 1976;14:1877–90.
- [6] Pecora R. *J Chem Phys* 1968;49:1032–5.
- [7] Ono K, Okano K. *Jpn J Appl Phys* 1971;9:1356.
- [8] Jones DR, Wang CH. *J Chem Phys* 1976;65:1835–40.
- [9] Wang CH, Fytas G, Lilge D, Dorfmueller Th. *Macromolecules* 1981;14:1363–70.
- [10] Johari GP. *Polymer* 1986;27:866–70.
- [11] Adachi K, Kotaka T. *Macromolecules* 1984;17:120–2.
- [12] Adachi K, Kotaka T. *Macromolecules* 1985;18:466–72.
- [13] Boese D, Momper B, Meier G, Kremer F, Hagenah JU, Fischer EW. *Macromolecules* 1989;22:4416–21.
- [14] Kanaya T, Patkowski A, Fischer EW, Seils J, Gläser H, Kaji K. *Acta Polym* 1994;45:137–42.
- [15] Kanaya T, Patkowski A, Fischer EW, Seils J, Gläser H, Kaji K. *Macromolecules* 1995;28:7831–6.
- [16] Pakula T. Simulation methods for polymers. In: Kotelyanskii MJ, Theodorou DN, editors. New York: Marcel-Dekker; 2004. p. 147–76.
- [17] Pakula T. Broadband dielectric spectroscopy. In: Kremer F, Schönhals A, editors. Berlin: Springer; 2002. p. 597–623.
- [18] Pakula T, Geyley S, Edling T, Boese D. *Rheol Acta* 1996;35:631–8.
- [19] Berne BJ, Pecora R. *Dynamic light scattering*. New York: Wiley; 1976.
- [20] Reiter J, Edling T, Pakula T. *J Chem Phys* 1990;93:837–44.
- [21] Gauger A, Weyersberg A, Pakula T. *Makromol Chem Theory Simul* 1993;2:531–60.
- [22] Mpoukouvalas K, Floudas G. *Phys Rev E* 2003;68(031801):1–7.
- [23] Fytas G, Patkowski A, Meier G, Fischer EW. *Macromolecules* 1988;21:3250–4.
- [24] Momper B. PhD thesis. University of Mainz; 1989.
- [25] Kriegs H, Gapinski J, Meier G, Paluch M, Pawlus S, Patkowski A. *J Chem Phys* 2006;124:104901–9.